Proceedings of the ASME/BATH 2014 Symposium on Fluid Power & Motion Control
FPMC2014
September 10-12, Bath, United Kingdom

FPMC2014-7856

EFFICIENCY TESTING OF AN ADJUSTABLE LINKAGE TRIPLEX PUMP

Shawn R. Wilhelm
University of Minnesota
Minneapolis, MN, USA

James D. Van De Ven
University of Minnesota
Minneapolis, MN, USA

ABSTRACT

Current state of the art variable displacement pumps suffer from poor efficiency at low volumetric displacement. Additionally, their performance is strongly dependent on operating conditions. A new variable displacement linkage pump architecture has been developed which can achieve high efficiency across a wide range of operating conditions. Previous work has described the kinematics, energy loss modeling, and experimental validation of a low power single cylinder prototype as well as the design of a second generation prototype. The second generation pump employs roller element bearings in its joints to minimize friction losses and the three cylinder design reduces the pressure ripple. In this paper, experimental characterization is presented of the new 21 MPa, 6.75 cc/rev pump. High mechanical efficiency is achieved at low volumetric displacements at partial loads as low as 0.6% of maximum power. Poorly performing cartridge check valves result in low volumetric efficiencies at low displacements. Close agreement was obtained between the model and predicted work input using measured cylinder data as an input into the model. This work shows that the presented pump with properly functioning valves can achieve high efficiency across a wide range of operating conditions. Having such versatile pump performance can greatly improve the performance of hydraulic systems as well as expand their potential applications.

INTRODUCTION

Variable displacement hydraulic pumps are used for applications that require a more efficient method of flow control than metering valves. A variable displacement pump can deliver the power required by the system, rather than throttling unnecessary power across a valve, thus consuming less energy to complete the same task. They are also used in pressure compensated systems in which the displacement control is used to maintain a constant system pressure.

The axial piston pump is the most widely used variable displacement machine due to its compact size and robust design. This pump uses a swash plate set at an angle to the rotational axis of a cylinder block. As the cylinder block rotates, the piston slippers slide along the swashplate on a hydrostatic bearing and the relative angle causes them to reciprocate. The angle of the swashplate determines the displacement of the pistons and is varied to adjust the pump output.

These pumps require a leakage path from the pumping cylinder to the swashplate in order to lubricate the piston-slipper joint and create the slipper-swashplate hydrostatic bearing. As a result, there are 3 leakage paths per piston with 9 or 11 pistons used in a typical pump. The leakage energy loss is relatively constant with respect to displacement.

Furthermore, the hydrostatic bearing between the swash plate and slippers results in viscous friction. The viscous friction energy loss increases with the square of the relative velocity, which in a typical application is constant and independent of displacement. Due to these constant energy loss terms, the efficiency of these pumps is poor at low output power [1]. Additionally, because the working fluid is also the lubrication fluid, applications of the axial piston architecture are primarily limited to non-corrosive fluids, unless exotic materials and coatings are used [2].

In an effort to design a pump which does not have the constant energy loss terms related to the piston-slipper interface, an adjustable linkage based pump has been developed which replaces the sliding joints with pin joints. Prior research has shown that a variable displacement linkage pump has the potential to have high efficiency across a wide range of displacements [3].

The linkage, depicted in Figure 1, consists of a base fourbar crank-rocker mechanism with an additional connecting rod-slider dyad, creating a sixbar mechanism. As the input crank rotates, it causes the rocker to oscillate. A connecting rod joins the rocker link to the piston at a common pin, resulting in reciprocation. The piston reciprocates in a cylinder, which uses check valves to cause a pumping action. The adjustable ground pivot the rocker is movable about a point, $\boldsymbol{p}$, associated with the top dead center position of the piston. By moving the adjustable ground pivot about this point, the displacement of the piston can be varied, while maintaining a constant top dead center. Additionally, placing the adjustable ground pivot along the sliding axis of the piston, results in zero piston displacement. A detailed description of the mechanism and associated kinematics can be found in [4, 5].

The constant top dead center position of the piston results in a constant, small dead volume, minimizing compressibility losses at all displacements. This in contrast to other designs where the dead volume increases with decreasing displacement, resulting in higher compressibility losses at lower power outputs. The zero displacement capability makes this pump infinitely variable, allowing for continuous input shaft rotation with no pumping output. The pin joints of the linkage allow for low friction rolling element bearings, the losses of which scale linearly with load and rotational speed.

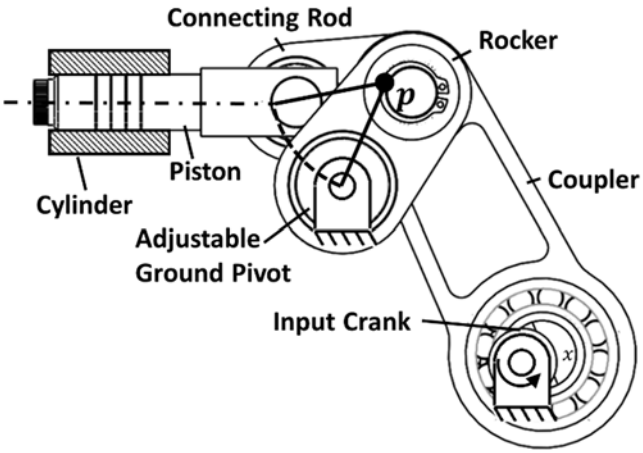

FIGURE 1 SCHEMATIC OF ADJUSTABLE LINKAGE SHOWING THE ADJUSTABLE GROUND PIVOT

As a result of these features, the majority of the energy losses of the adjustable linkage mechanism scale with displacement and the mechanical efficiency remains relatively constant for a majority of the displacement range. Additionally, because hydrostatic bearings are not required, the lubricating fluid can be separated from the pumping fluid using positive seals, as is commonly practice for fixed displacement linkage type pumps. The design can be used for a wide range of applications and multiple leakage paths are eliminated. A model validation for a low power, single cylinder pump using bronze sleeve bearings was previously conducted [6]. This work showed close agreement between model and experiments and concluded that the efficiency could be greatly improved if roller element bearings are used in the pump.

A new, three-cylinder prototype, which uses roller element bearings, has been constructed for model validation. The pump is designed to operate at 21 MPa and 3600 rpm, with a maximum displacement of 6.75 cc/rev. Check valves were used for flow control for design simplicity. The displacement mechanism is the focus of this paper as the volumetric performance depends heavily on the performance of the valve mechanism which is under separate development and requires special attention.

A multi-objective genetic algorithm was used to optimize the dimensions of the linkage and pumping chamber to maximize efficiency and minimize pin forces. The bearings were selected for a 10 khr operating life at peak load conditions. This life was calculated from bearing catalog design equations for both oscillating and rotary motion depending on the installed joint. A crosshead bearing was not used in this design because the piston side loading was relatively small reducing the overall size. A previous work describes the design and optimization of the machine [3].

In this paper, the three-cylinder pump model will be experimentally validated and experimental efficiency data is presented. Testing equipment and valve limitations prevented operating the pump at full capacity, so low power data is provided here. It will be shown that high mechanical efficiencies can be achieved at low displacement. The paper is split into five sections. First the energy loss model is presented. Second the experimental methods are presented including the prototype and experimental setup. Third, the results of the experiments are given. The fourth section provides discussion and the fifth section gives conclusions.

NOMENCLATURE

A_p	$Piston\ cross\ sectional\ area\ [m^2]$
d_p	$Piston\ diameter\ [m]$
D	$Pump\ Displacement\ \left[\frac{m^3}{rev}\right]$
E_{cf}	$Energy\ of\ coulomb\ friction\ [J]$
E_{ql}	$Energy\ of\ leakage\ flow\ [J]$
E_v	$Energy\ of\ viscous\ friction\ [J]$
F_N	$Normal\ Force\ of\ Pin\ Joint\ [N]$
F_{N_c}	$Normal\ Force\ on\ Piston\ Joint\ [N]$
T_{cf}	$Coulomb\ frictional\ Torque\ [J]$
E_β	$Energy\ of\ fluid\ compresibility\ [J]$
F_v	$Viscous\ friction\ force\ [N]$
h	$Piston\ cylinder\ gap\ height\ [m]$
l_p	$Piston\ length\ [m]$
P_{sys}	$System\ Pressure\ [Pa]$
$\boldsymbol{p}$	$Location\ of\ Adjustment\ Pivot\ (complex)\ [m]$
Q_{leak}	$Leakage\ flow\ rate\ \left[\frac{m^3}{s}\right]$
Q	$Flowrate\ from\ pump\ \left[\frac{m^3}{s}\right]$
r	$Radius\ of\ pin\ [m]$
T	$Linkage\ input\ torque\ [Nm]$
V_{dead}	$Unswept\ Cylinder\ Volume\ [m^3]$
v_{S_i}	$Velocity\ of\ the\ i^{th} piston\ \left[\frac{m^3}{s}\right]$
β	$Compressibility\ of\ the\ working\ fluid\ [Pa]$
η_m	$Mechanical\ Effiency\ [unitless]$
η_{pump}	$Efficiency\ of\ pump\ [unitless]$
η_v	$Volumetric\ Efficency\ [unitless]$
μ_d	$Dynamic\ viscosity\ of\ working\ fluid\ [Pa\ s]$
μ_k	$Dynamic\ friction\ coefficient\ [unitless]$
μ_{kc}	$Dynamic\ friction\ coefficient\ [unitless]$

ω $\quad$ $Angular\ velocity\ input\ shaft\ \left[\frac{rad}{s}\right]$

ENERGY LOSS MODELING

There are four energy losses modeled, including viscous friction in the piston cylinder interface, coulomb friction in the pin joints, leakage between the piston cylinder, and compressibility losses due to the dead volume. For this model, it is assumed that the losses related to eccentricity relative to the cylinder are negligible as shown by Kumar [7], and as a result, the piston-cylinder clearance is considered constant. Ridges are added to the piston to aid in maintaining concentricity. The working fluid is considered Newtonian with fully developed, laminar flow in the piston-cylinder gap. Isothermal operation is assumed. Additionally, input shaft seal friction and splash lubrication energy are not considered. The check valves are not modeled, as the work presented here pertains to the pumping mechanism and the valves are considered outside the scope of the current work.

Viscous Friction Energy Losses

Viscous friction is cause by the relative motion between the piston and cylinder, resulting in shearing of the fluid in the gap between the two. The viscous friction force is described by Newton's law of viscosity:

$$F_v = \pi d_p l_p \frac{\mu_d}{h} v_s \quad (1)$$

where d_p is the piston diameter, l_p is the piston length, μ_d is the dynamic viscosity of the fluid, h is the radial piston clearance, and v_s is the relative velocity of the piston and cylinder. The energy loss due to viscous friction is expressed as:

$$E_v = \int F_v dx = \int F_v v_s dt \quad (2)$$

Coulomb Friction Energy Losses

Rolling friction occurs in the bearings of the mechanism as the inner race rotates relative to the outer race. A Coulomb friction model is used to calculate the friction energy using an equivalent coefficient of friction, μ_{rb}. The friction energy loss over a cycle is found by integrating the friction torque with respect to the angle of rotation between the pin and the link:

$$T_{cf} = \mu_k F_N r_{rb} \quad (3)$$

$$E_{cf} = \int T_{cf} d\theta_j = \int T_{cf} \omega_j dt \quad (4)$$

where T_{cf} is the resultant friction torque which opposes the direction of motion at the outer surface of the pin, F_N is the magnitude of the force applied to the joint, r_{rb} is the equivalent radius of the pin as described by Beardmore [8], $d\theta_j$ is the relative change in angle between the link joint and the pin, and ω_j is the relative angular velocity between the link joint and the pin. The friction energy loss is calculated for each bearing in the linkage and summed to determine the total roller bearing energy loss of the mechanism. In addition to the coulomb friction in the pin joints, there is additional friction loss at the crosshead bearing, described by:

$$F_{cf_{crosshead}} = \mu_{kc} F_{Nc} \quad (5)$$

$$E_{cf_{crosshead}} = \int F_{cf} v_s dt \quad (6)$$

Piston-Cylinder Leakage Energy Losses

The gap between the piston and cylinder allows leakage flow as a result of a pressure drop across the piston. As described by Cundiff, the leakage flow rate for a piston clearance seal is [9]:

$$Q_{leak} = \frac{\pi d_p h^3}{12 \mu_d l_p} P_{cyl_i} \quad (7)$$

The energy loss associated with this leakage is calculated by integrating the leakage flow with respect to time:

$$E_{ql} = \int \mathrm{P_{cyl_i}} Q_{leak} dt \quad (8)$$

Fluid Compressibility

The working fluid of the pump is compressible, as described by the bulk modulus, β. As the cylinder is presurized there is a resulting compression of the working fluid, causing energy to be stored and then released when cylinder pressure is reduced. The energy loss associated with fluid compressibility over a cycle is given as:

$$E_\beta = \frac{\Delta P^2 V_{dead}}{\beta} \quad (9)$$

where ΔP is the change in pressure, V_{dead} is the unswept chamber volume, and β is the bulk modulus of the fluid. If active valves are used, the compression energy of the fluid in the unswept volume results in an energy loss. Because passive valves are used in the presented prototype, this energy is recoverable and not considered here. Additionally, because the pump has a small, constant, unswept volume, this loss is insignificant with respect to the other energy loss mechanisms and can be considered negligible.

Figure 2 shows the modeled energy loss contibutions for the optimized pump as a function of displacement for a single cylinder at 21 MPa and 60 Hz operating frequency. The roller bearing friction dominates. Due to the optimized piston-cylinder gap height of 20 μm, the leakage and viscosity terms are fairly similar. The compressibility losses are negligible in comparison to the other contributions.

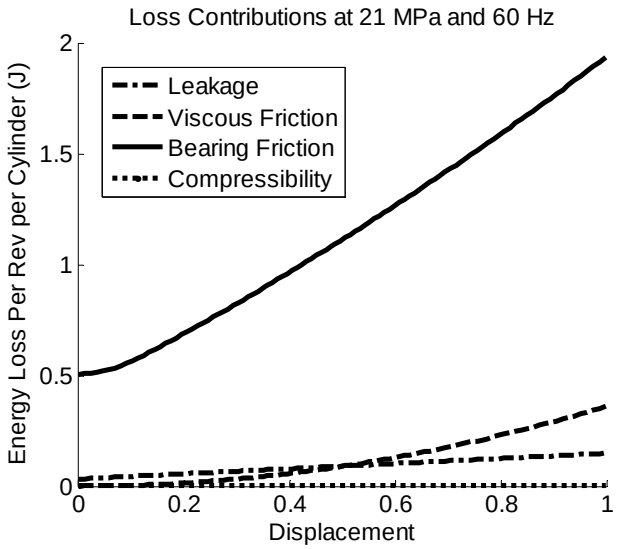

FIGURE 2 MODEL PREDICTED ENERGY LOSS CONTRIBUTIONS OF A SINGLE CYLINDER AT 60 HZ AND 21 MPA OPERATION PLOTTED VS DISPLACEMENT

METHODS

The pump efficiency is determined using the experimental setup depicted in Figure 3. The pump is driven by a 3-phase electric motor with a variable frequency drive to control shaft speed. A pilot operated relief valve provides both a pressure control and a load. The displacement is measured with an absolute encoder placed on the control link. A hydraulic actuator is used to vary the pump displacement, and is powered by the pumps own output through a directional control valve. The input power is calculated from the shaft speed, which is measured using an optical encoder, and the torque, which is measured using an inline rotary torque transducer. Output power is calculated using a pressure transducer at the pump outlet and a gear flow meter.

Three additional pressure transducers are used to monitor each cylinder for evaluating pumping performance and determining piston loads for model comparison. The optical encoder was also used to estimate piston position by measuring the encoder count relative to the piston position. For calibration, the pump was partially disassembled to directly measure the piston position using an LVDT relative to the position of the optical encoder on the input shaft.

A 1 liter accumulator pre-charged to 1.7 MPa is connected to the outlet of the pump, before the flow meter to reduce flow ripple. Eaton CV3-10-003 poppet check valves were used on the pumping chamber outlets and disk style check valves from a commercial pump were used on the inlets. The disk check valves were selected for the inlet due to their fast response time and low cracking pressure.

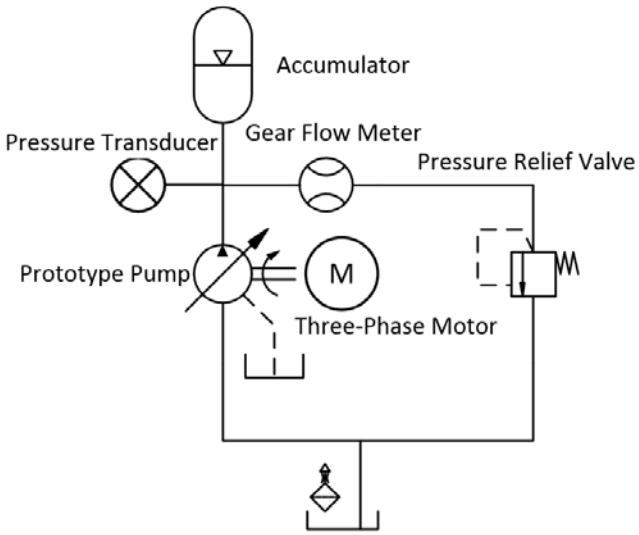

FIGURE 3 SCHEMATIC OF THE EXPERIMENTAL TEST SETUP

In a given set of experiments, the shaft speed is set, followed by pressure. Then the pump is set to maximum displacement. For each test, the system is given 30 seconds to reach cyclic steady state, at which point the accumulator is not storing or supplying energy over the course of a cycle. Data is then collected for five seconds and the displacement is then reduced to the next set point. Ten displacements are measured per pressure and speed setting. The working fluid is ISO grade 46 hydraulic fluid.is used at a working fluid with the temperature maintained at 22-25° C.

As of the time of publication the pump has been tested to a maximum of 7 MPa. The pumping frequency was limited to 10 Hz by the response time of the commercially available poppet style cartridge check valves used in the manifold block.

Figure 4 is a plot of the pressure volume trace of a single cylinder at 10 Hz, 6 MPa, and 60% displacement, demonstrating the effective portion of the stroke. The volume is calculated from the measured piston position and the cylinder pressure is measured with the cylinder pressure transducer. The lag in opening of the check valve is demonstrated by the slope of the rise and fall of pressure and is an indication of the valve performance. Ideally, the rise and fall for an incompressible fluid would be vertical lines. Due to the slow performance of the valves, the ideal valve model could not be used for model predictions.

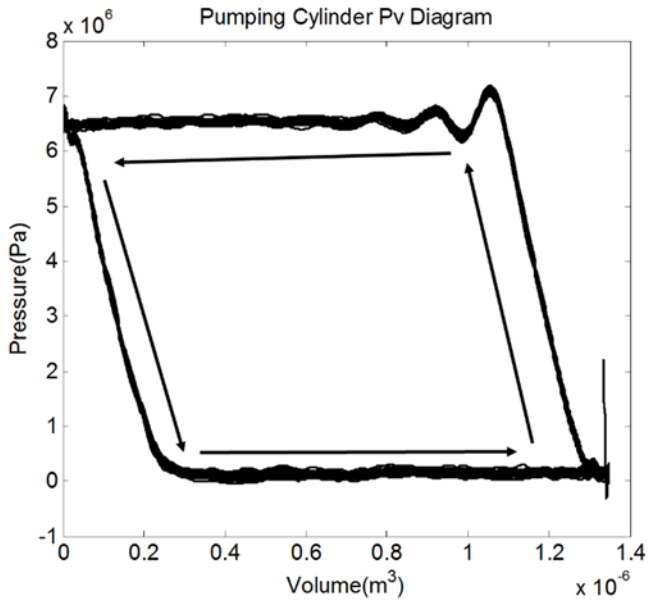

FIGURE 4 EXPERIMENTALLY MEASURED PRESSURE VS. VOLUME DIAGRAM OF PUMPING CYLINDER WITH ARROWS INDICATING CYCLE DIRECTION

The measured system pressure, flow rate, input torque, and shaft speed are used to directly calculate mechanical, volumetric, and total efficiencies. Mechanical efficiency is defined as:

$$\eta_m = \frac{P_{sys} D}{2\pi T \omega} \tag{10}$$

where P_{sys} is the average system pressure, D is the total volume swept by the three pistons per revolution, T is the average input torque, and ω is the average shaft speed.
The volumetric efficiency is defined as:

$$\eta_v = \frac{2\pi Q}{D\omega} \tag{11}$$

where Q is the averaged flow rate. All measured values are averaged over the five second experiment. Total efficiency is defined as:

$$\eta_{pump} = \frac{P_{sys} D}{T\omega} = \eta_m \eta_v \tag{12}$$

For model comparison, the experimental cylinder pressure and piston position are used as inputs to the kinematic model presented in [6], including the losses mentioned in the modeling section. Figure 5 shows a plot of the experimentally measured torque compared to the model predicted torque at 10 Hz, 6 MPa, and 60% displacement. The torque predicted by the model agrees well with the experimental data.

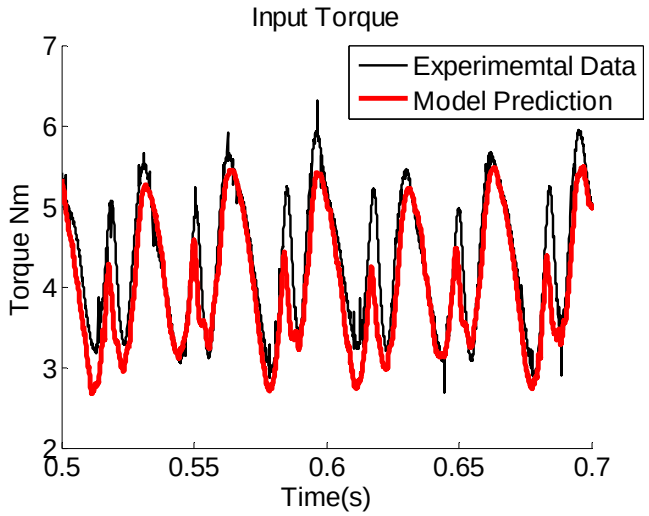

FIGURE 5 MODEL PREDICTED VS EXPERIMENTALLY MEASURED INPUT TORQUE USING CYLINDER PRESSURE AS AN INPUT TO THE MODEL AT 10 HZ 6 MPA AND 60% DISPLACEMENT

RESULTS

The mechanical efficiency of the pump was greater than 90% at all measured displacements at pressures above 5 MPa and shaft speeds above 600 RPM. The highest mechanical efficiency measured was 98% at 7 MPa and 40% displacement. These data are shown in Figure 6, which is a plot of mechanical efficiency as a function of displacement, with multiple traces to represent different operating pressures. The mechanical efficiency trends upwards with increased pressure while the volumetric efficiency trends down with increased pressure as shown in Figure 7.

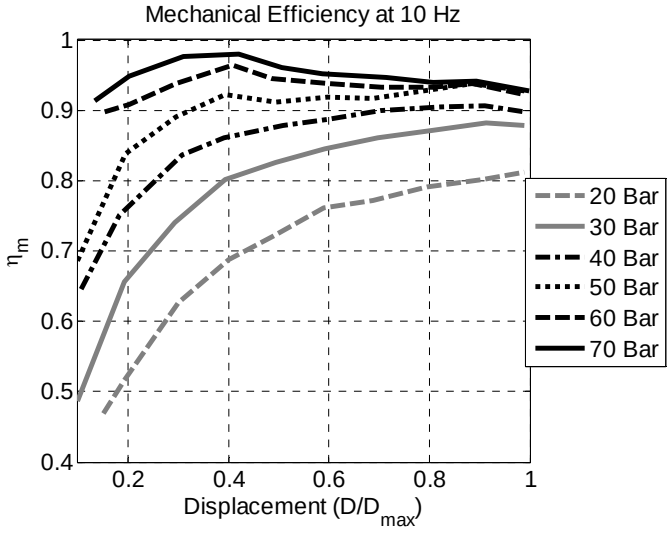

FIGURE 6 EXPERIMENTALLY MEASURED MECHANICAL EFFICIENCY PLOTTED AGAINST DISPLACEMENT AT 10 HZ OPERATING SPEED AT VARIOUS OPERATING PRESSURES

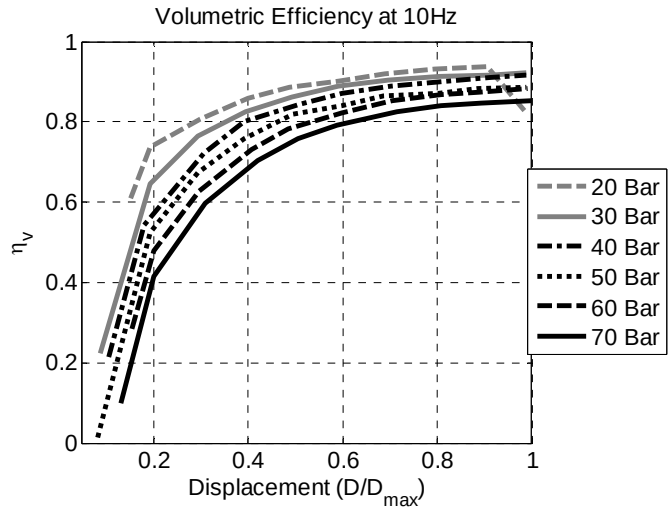

FIGURE 7 EXPERIMENTALLY MEASURED VOLUMETRIC EFFICIENCY PLOTTED AGAINST DISPLACEMENT AT 10 HZ OPERATING SPEED AT VARIOUS OPERATING PRESSURES

As seen in Figure 8, when the experimentally measured piston position, cylinder pressure, and shaft speed are passed as inputs to the model, the input shaft work well is well predicted.

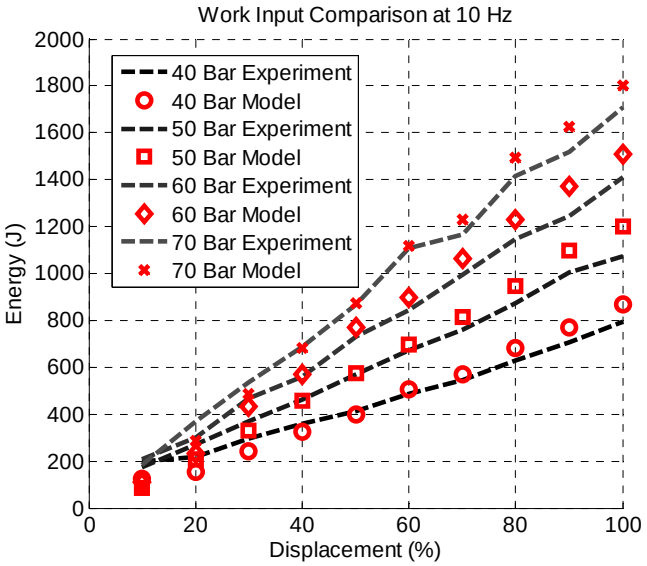

FIGURE 8 COMPARISON OF MODEL PREDICTED AND EXPERIMNETALLY MEASURED INPUT WORK USING EXPERIMENTAL CYLINDER DATA AS AN INPUT TO THE MODEL

DISCUSSION

Slow check valves prevented the pump from producing the expected total efficiencies and reaching higher operating speeds. This is shown in the volumetric efficiency measurement. However, the mechanical efficiency was high even at low displacements. These measurements are taken at partial loads of 0.3-6% of the design power, which is encouraging for the performance at higher power levels. Additionally, the experimental data matches closely with the model when taking valve timing into account across a broad range of operating conditions. This close agreement shows that the model can predict well how the mechanism will perform as a function of the pumping head behavior.

Having a pump with such high efficiency at low displacements is an exciting prospect for current hydraulic applications. Additionally, because the pump allows for the separation of the working fluid from the lubrication fluid, the potential for new applications is great.

According to a report by Oak Ridge National Labs, the average efficiency of industrial hydraulics systems is ~50%, consuming 3% of the total energy use in the United States. They concluded that the inefficiencies were largely a result of the use of metering valves [10]. These losses can be greatly reduced by using variable displacement flow control.

For many industrial applications, traditional variable displacement pumps cannot be used to control flow rates because the working fluid is not lubricating. Variable frequency drives are used in some cases, but they add extra components to the system and can cause premature wear in electric motors. [11]. However, this new pump can be used in such cases to eliminate metering valves, and vastly improve the efficiency of these systems.

Additionally, this pump could be used to reduce energy consumption and allow for non-lubricating working fluid in applications which currently use variable displacement pumps. For example, an injection molding machine could use water hydraulics which would aid in heat transfer while consuming less energy.

Further work is required to increase the power density of this new pump design to make it more viable for mobile applications which have strict size restrictions.

In the future, a new power supply will be used to evaluate the pump at its full operating range to further validate the capabilities. Additional work is required to create high speed, low inertia check valves which will allow higher frequency operations and prevent reverse flow at low displacements.

CONCLUSIONS

A prototype adjustable linkage pump, which uses roller element bearings in its joints, demonstrated mechanical efficiencies greater that 90% as partial loads as low as 0.6%. The volumetric efficiency of the presented prototype was limited by poorly performing check valves, but the model was still able to predict the mechanisms behavior.

The variable displacement linkage pump is able to eliminate the leakage and friction losses associated with the hydrostatic bearings by using all rolling element bearings. This paper validates the energy loss models of the bearing friction and leakage. Energy losses associated with bearings were reduced by approximately ten times when compared to the previously presented bronze bushing design, proving their added value.

Work is already underway to incorporate high speed check valves into the design allowing for this pump to achieve its full potential. In the future, active valves will also be incorporated to allow for motoring operation.

ACKNOWLEDGMENTS

This work is supported by the National Science Foundation under grant number EFRI-1038294.

REFERENCES

[1] Wilson, W., 1946, "Rotary-pump theory," Trans. ASME, 68(4), 371-384.
[2] Haynes, J. M., 2007, "Axial piston pump leakage modelling and measurement," PhD, Cardiff University.
[3] Wilhelm, S. R., and Van de Ven, J. D., 2014, "Design of a Variable Displacement Triplex Pump," International Fluid Power ExpositionLas Vegas, NV.
[4] Wilhelm, S. R., and Van de Ven, J. D., 2013, "Design and Testing of an Adjustable Linkage for a Variable Displacement Pump," Journal of Mechanisms and Robotics, 5(4), 041008.
[5] Wilhelm, S., and Van de Ven, J. D., 2011, "Synthesis of a Variable Displacement Linkage for a Hydraulic Transformer," International Design Engineering Technical Conferences & Computers and Information in Engineering Conference, ASME, Washington, DC, 8.
[6] Wilhelm, S. R., and Van de Ven, J. D., 2013, "Efficiency Modeling and Experimental Validation of a Variable Displacement Linkage Pump," ASME/BATH Symposium on Fluid Power and Motion Control, ASME, Sarasota, FL.
[7] Kumar, S., 2010, CFD Analysis of an Axial Piston Pump, PhD Thesis from UPC, Spain.
[8] Beardmore, R., 2010, "Roller Bearing Friction," http://www.roymech.co.uk/Useful_Tables/Tribology/Bearing%20Friction.html.
[9] Cundiff, J. S., 2002, Fluid Power Circuits and Controls: Fundamentals and Applications, CRC Press.
[10] Love, L., Lanke, E., and Alles, P., 2012, "Estimating the Impact (Energy, Emissions and Economics) of the US Fluid Power Industry," Oak Ridge National Laboratory (ORNL).
[11] 2000, "Variable Frequency Drives," No. 00-054, Easton Consultants, Inc. .